THE JOURNAL OF PHYSICAL CHEMISTRY C

Article

pubs.acs.org/JPCC

Manipulating the Conformation of Single Organometallic Chains on Au(111)

Alex Saywell,[†] Wojciech Greń,[‡] Grégory Franc,[‡] André Gourdon,[‡] Xavier Bouju,[‡] and Leonhard Grill*[,†,§]

[†]Department of Physical Chemistry, Fritz-Haber-Institute of the Max-Planck Society, 14195 Berlin, Germany

[‡]Nanosciences Group, CNRS, CEMES, 29 Rue J. Marvig, 31055 Toulouse, France

[§]Department of Physical Chemistry, University of Graz, Heinrichstrasse 28, 8010 Graz, Austria

Supporting Information

ABSTRACT: The conformations of organometallic polymers formed via the bottom-up assembly of monomer units on a metal surface are investigated, and the relationship between the adsorption geometry of the individual monomer units, the conformational structure of the chain, and the overall shape of the polymer is explored. Iodine-functionalized monomer units deposited on a Au(111) substrate are found to form linear chain structures in which each monomer is linked to its neighbors via a Au adatom. Lateral manipulation of the linear chains using a scanning tunneling microscope allows the structure of the chain to be converted from a linear to a curved geometry, and it is shown that a transformation of the overall shape of the chain is coupled to a conformational rearrangement of the chain structure as well as a change in the adsorption geometry of the monomer units within the chain. The observed conformational structure of the curved chain is well-ordered and distinct from that of the linear chains. The structures of both the linear and curved chains are investigated by a combination of scanning tunneling microscopy measurements and theoretical calculations.

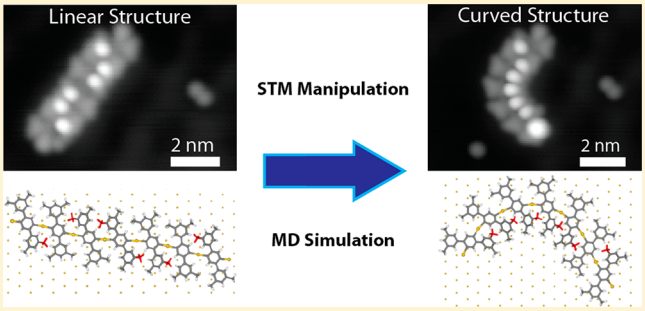

INTRODUCTION

Scanning tunneling microscopy (STM) can be used to both image and manipulate individual atoms[1−4] and molecules[5−13] that are confined on a substrate held under ultrahigh vacuum (UHV) conditions. The manipulation of rigid molecules has previously been studied and has allowed molecular motions such as pushing, pulling, hopping, and rolling modes to be investigated.[3,9,10] Moreover, the study of conformational changes within single molecules has revealed insight into their internal flexibility and mobility.[11−13] However, the single-molecule manipulation of more complex structures (i.e., with more conformational flexibility), for example, the bending of chains on a surface, is less well-studied.[14−17] This is mainly due to the difficulties in depositing such large molecules on surfaces in a clean and intact fashion;[18] hence, alternative strategies such as the on-surface formation of organometallic[19−21] or covalently bonded structures[22] are utilized. Although the adsorption geometry of monomers within a Cu-coordinated polymer has been studied,[23] no details of the manipulation of the conformational structure of a molecular chain or the interaction between the conformation of the chain and its overall shape have been reported. Here we investigate the structure and conformations of a flexible self-assembled molecular chain formed from metal−organic linkages between gold atoms and precursor monomer units. The structures are formed in situ by an on-surface chemical reaction leading to the formation of molecular chains that show a correlation between the adsorption geometry of the individual monomer units and the conformation and large-scale structure of the chain. The low-temperature STM (LT-STM) results presented here demonstrate that it is possible to mechanically induce a transition of a molecular chain from a linear to a curved structure with the STM tip and that such a transition has an effect on the conformational structure of the chains.

EXPERIMENTAL DETAILS AND CALCULATION METHODS

Synthesis of 2′,5′-diiodo-3,3″,5,5″-tetramethyl-1,1′:4′,1″-terphenyl (I_2TMTP). The monomer was prepared by the reaction of 1,4-dibromo-2,5-diiodobenzene with (3,5-dimethylphenyl)-magnesium bromide and quenching of the di-Grignard intermediate with iodine according to a procedure similar to that reported in a previous study.[24] A solution of 1,4-dibromo-2,5-diiodobenzene (500 mg, 1.025 mmol) in 4 mL of dry THF was added slowly over 30 min to a solution of xylene magnesium bromide (C = 0.5 M in THF, 4.10 mmol); the resulting mixture was stirred for an additional 2 h at room temperature. The reaction mixture was then cooled to 10 °C and 5.1 g (20 mmol) of iodine was added; the resulting mixture

Received: September 18, 2013
Revised: October 23, 2013
Published: October 24, 2013

   dx.doi.org/10.1021/jp409323g | J. Phys. Chem. C 2014, 118, 1719−1728

was stirred at 10 °C for 1 h. It was then quenched with ice–water and extracted with DCM, and the organic layer was dried and evaporated under reduced pressure. HPLC led to the final compound as a white solid (90 mg; 16%). 1H NMR (300 MHz, $CDCl_3$): δ = 2.39 (s, 12H, CH_3); 6.98 (s, 4H, Har); 7.05 (s, 4H, Har); 7.83 (s, 2H, Har).

STM experiments were performed under UHV conditions (base pressure 10^{-10} mbar), with a separate chamber (base pressure 10^{-9} mbar) used for the preparation of the sample. A Au(111) sample (MaTecK GmbH) was cleaned by argon ion sputtering (2 keV, I_{sample} = ~4.5 μA, P_{Ar} = ~5 × 10^{-6} mbar, 25 min) and subsequent annealing at ~400 °C for 10 min. STM images were obtained at temperatures of about 6 K with a modified Omicron LT-STM (with Nanonis Electronics). The STM was operated in constant current mode, and electrochemically etched tungsten tips were used, which were probably covered with gold from many routine indentations into the surface for tip optimization. I_2TMTP was deposited from a Knudsen-cell-type evaporator (Kentax GmbH) at about 120 °C.

The energies and optimized geometries for the molecular structures were obtained by force-field-based molecular mechanics (MM) and dynamics (MD) calculations, which were performed within the DL_POLY code.[25,26] The parameters for intramolecular interactions were taken from the DREIDING generic force field,[27] and the Sutton and Chen potential[28] was used to parametrize the interactions between the gold atoms. The interactions between the I_2TMTP oligomers and the surface were described using parameters derived by Johnston and Harmandaris.[29] The parameters for describing organometallic bonds were adapted from the DREIDING model with the equilibrium bond length, bond angles, and torsional angles being obtained from DFT calculations (see Supporting Information for details). The optimized structures were obtained by implementing a simulated annealing process with a MD simulation performed at 300 K for 1 ns and then quenched to obtain the energy-minimized structures. The barriers between local minima were calculated using constrained minimization (at least one degree of freedom of an atom in the molecule is kept fixed, with all other degrees of freedom allowed to relax) and the nudged elastic band method.[30]

The calculated STM images were produced using the elastic scattering quantum chemistry (ESQC) technique,[31,32] which has demonstrated its efficiency and reliability to perform accurate STM image calculations of various chemical systems ranging from atoms[33] to large molecules.[34] In this method, the transmission coefficient of electrons moving through the STM junction is calculated and the Landauer formula[35] is used to obtain the tunneling current. The atoms in the junction were described by taking into account their full valence structure. Full details are given in the Supporting Information.

RESULTS AND DISCUSSION

The monomer unit studied here is I_2TMTP (2′,5′-diiodo-3,3″,5,5″-tetramethyl-1,1′:4′,1″-terphenyl; structure shown in Figure 1a), which consists of a flexible *p*-terphenyl backbone with the two terminal aryl rings functionalized with two methyl groups at the *meta* positions and two iodine atoms on the central aryl ring. The carbon–iodine bond within an organic molecule is known to dissociate upon adsorption on Au, Ag, and Cu surfaces at room temperature, as has been shown for various molecules.[15,36−38] This leads in general to a second reaction step, the intermolecular Ullmann carbon–carbon coupling.[15,16,22,36,39−45]

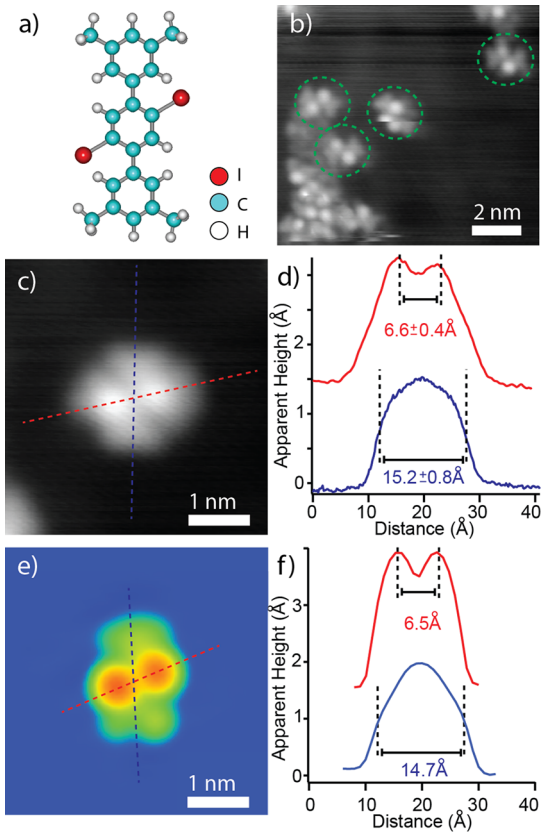

Figure 1. (a) Chemical structure of the I_2TMTP molecule. STM images of (b) the Au(111) surface after deposition of I_2TMTP (surface cooled to ~30 K during deposition, $V_{tip\text{-}bias}$ = −100 mV, I_{tunnel} = 100 pA) and (c) a single I_2TMTP molecule with the position of two line profiles indicated ($V_{tip\text{-}bias}$ = −500 mV, I_{tunnel} = 100 pA). (d) Two line profiles showing the peak-to-peak separation between the iodine atoms and the FWHM length of the molecule. (e) ESQC-calculated STM image of a single I_2TMTP molecule adsorbed on the Au(111) surface. (f) Line profiles from (e) showing the calculated iodine–iodine separation and the FWHM length of the calculated molecule.

Here, our initial aim was to utilize an on-surface chemical reaction to produce covalently bonded linear polymers. To characterize the structure of the unreacted monomer units, the I_2TMTP molecule was deposited on a Au(111) sample held at a temperature of approximately 30 K with the C–I bond expected to remain intact upon molecular adsorption because of the low temperature.[15] The sample was then transferred to the LT-STM for analysis (during the transfer the maximum temperature of the sample is expected to stay below 45 K). A typical image of the resulting surface is shown in Figure 1b in which 4 "bow-tie" like features, attributed to the monomer species, are highlighted by green dashed ellipses. The structure of the molecule consists of two slightly offset bright white lobes in the center of each molecule and two roughly triangular features at the ends of the long-axis of the molecule. Note that the I_2TMTP molecule in the center of the image (Figure 1b) appears in a discontinuous fashion, assigned to molecular motion induced by the tip during scanning due to the much smaller time scales of the motion as compared to those of the scanning procedure that are in the range of seconds and minutes.

dx.doi.org/10.1021/jp409323g | J. Phys. Chem. C 2014, 118, 1719−1728

A close-up STM image of a monomer (Figure 1c) shows in more detail the positions of the two bright lobes. Line profiles across the molecule (Figure 1d) reveal that the separation between the two bright protrusions within the I_2TMTP molecule is 6.6 ± 0.4 Å (averaged over many molecules) and that the length of the molecule (determined from the full width at half-maximum (FWHM) of the height profile) is 15.2 ± 0.8 Å. Both values agree well with the theoretical values of 6.5 and 14.7 Å, respectively, obtained from a combination of density functional theory (DFT), geometry optimization, and calculated STM images (the calculated STM images shown in Figure 1e,f were produced using the ESQC technique[31]). This demonstrates that the bright protrusions can be directly attributed to the iodine atoms as part of the molecular structure and that both of the C−I bonds are, as expected, intact after deposition of the molecule as the catalytic activity is suppressed on the cold surface. The symmetric appearance of the molecule indicates that it is lying flat on the Au(111) surface with both of the dimethyl-aryl rings lying parallel to the surface plane. The apparent height of the flat lying dimethyl-aryl rings is measured to be 0.8 ± 0.3 Å, and the apparent height of the iodine atoms is found to be 1.1 ± 0.3 Å.

Depositing I_2TMTP onto a Au(111) surface held at room temperature, followed by annealing at 120 °C for 10 min, leads to a different result. Linear chains are formed (Figure 2a), which are observed to run along the close-packed $\langle 1\bar{1}0 \rangle$ directions of the surface and disrupt the underlying herringbone reconstruction,[46] pointing to a relatively strong molecule−surface interaction. This is in contrast to similar experiments involving the on-surface synthesis of molecular architectures using Br functionalized moieties where the reconstruction is still present.[16,42,43] Figure 2b shows a close-up of a linear chain with several features indicated (A−C). A are identified from their nearest neighbor separation (approximately 5.0 Å; see Figure S15 of the Supporting Information) as iodine atoms which, as expected, have dissociated from the monomer unit because of the catalytic activity of the surface.[15,36] These atoms are free to diffuse at the annealing temperature of 120 °C, as evidenced by the formation of close-packed islands with dimensions identical to those observed by Huang et al. for the low coverage $(\sqrt{3} \times \sqrt{3})R30°$ structure of iodine deposited on Au(111)[47] (see Supporting Information for extended discussion). The apparent height of the iodine features is measured to be 1.2 ± 0.1 Å.

For the low temperatures at which the STM images are acquired, the iodine atoms are not diffusing and are found at elbow sites on the herringbone reconstruction or form close-packed structures close to molecular chains. In addition, two well-defined features can be identified along the length of the linear chains; these are the bright protrusions (B) and the darker features (C). Their apparent heights (2.4 ± 0.2 and 1.4 ± 0.1 Å for B and C, respectively) are found to be independent of their position along the chain. An important characteristic is that the bright features, B, form a highly regular structure with pairs of bright lobes alternating along opposite sides of the long axis of the chain (Figure 2c). The experimentally measured periodicity, L_0^{Exp}, of this structure is 28 ± 1 Å, which is surprisingly large compared to the small separation between the monomer units (4.6 Å for a covalently bonded chain, see below). Such a long-distance periodic arrangement of the internal structure indicates a rather complex interaction between the monomer units, as a simple nearest-neighbor interaction model where neighboring units may exist in only one of two states (bright or dark) would not account for the observed periodicity with a length approximately six time greater than the intermolecular separation. Three distinct

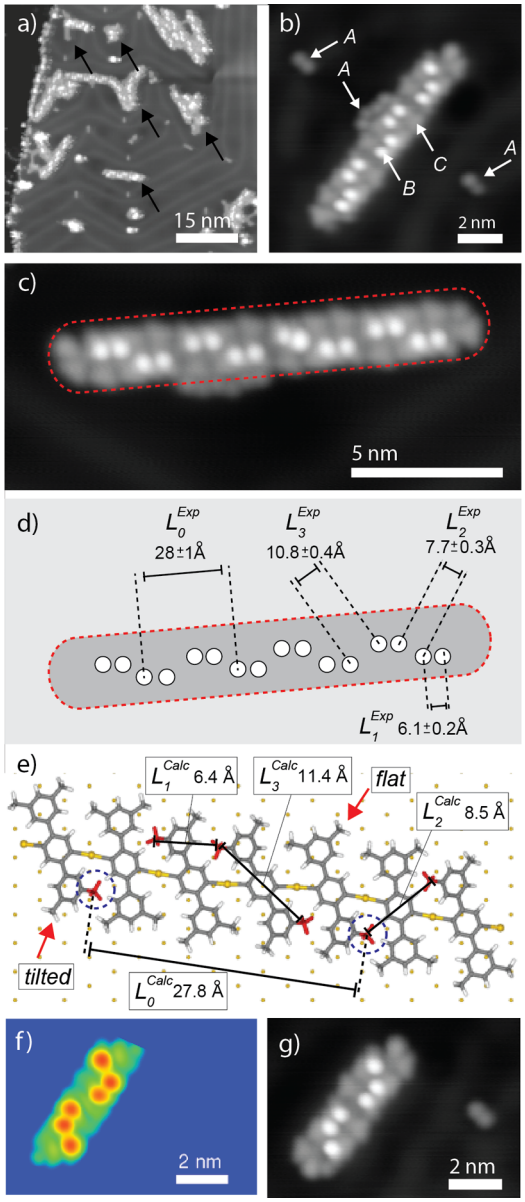

Figure 2. (a) STM image of the Au(111) surface with self-assembled chains of TMTP monomers: deposition with the sample held at RT, followed by annealing at 120 °C for 10 min. Arrows indicate regions of disrupted herringbone reconstruction ($V_{tip\text{-}bias}$ = −1000 mV, I_{tunnel} = 10 nA). (b) STM image showing a close-up of a linear TMTP chain ($V_{tip\text{-}bias}$ = +50 mV, I_{tunnel} = 300 pA). Several features are indicated: A, iodine adatoms; B, bright feature of a TMTP monomer; C, dark feature of a TMTP monomer. (c) STM image showing the highly periodic internal structure of a linear TMTP chain on the Au(111) surface ($V_{tip\text{-}bias}$ = −1000 mV, I_{tunnel} = 10 nA). (d) Schematic diagram highlighting the periodicity of the bright features within the linear TMTP chain. The dimensions for the periodicity (L_0^{Exp}) and the three distances between the bright features (L_1^{Exp},L_2^{Exp}, and L_3^{Exp}) are indicated. (e) Molecular mechanics (MM) simulation of a linear TMTP chain. The dimensions for the periodicity (L_0^{Calc}) and the three distances between the terminal methyl groups (L_1^{Calc}, L_2^{Calc}, and L_3^{Calc}) are indicated. (f) ESQC-calculated STM image of the linear TMTP chain from the calculated structure shown in (e). (g) STM image showing a linear TMTP chain ($V_{tip\text{-}bias}$ = −100 mV, I_{tunnel} = 100 pA).

dx.doi.org/10.1021/jp409323g | J. Phys. Chem. C 2014, 118, 1719−1728

distances for the separation between neighboring bright features can be measured (labeled L_1^{Exp}, L_2^{Exp}, and L_3^{Exp} in Figure 2d).

To gain understanding of the complex internal structure of the polymer chains, molecular mechanics (MM) geometry optimization calculations as well as ESQC calculations were performed. Various covalently bonded molecular architectures have been formed by on-surface synthesis based on the Ullmann coupling in the last years,[15,16,22,36,39−45] and because of the presence of halogen substituents, this can also be expected in the present case. However, we find that the dimensions of a polymer structure based upon covalently linked monomer units (4.6 Å separation between neighboring dimethyl-aryl rings, determined by MM calculations) are substantially smaller than the experimentally observed separation of 6.1 ± 0.2 Å between neighboring monomers, indicating that the monomer units are not bound via a C−C covalent bond. In addition, the corresponding calculated STM image for the covalently bonded chain disagrees qualitatively with the experimental data, with the periodic appearance of pairs of bright features not observed in the calculated images (see Supporting Information Figures S5 and S6 for an extended discussion). We find instead that a structural model in which the monomer units are connected by metal−organic bonds is in very good agreement with our experimental results. Figure 2e shows the MM-geometry-optimized structure for a linear chain consisting of seven monomer units connected by metal−organic linkages, i.e., C−Au−C bonds. Similar organometallic structures have previously been observed to exist as stable intermediates of the Ullmann coupling reaction,[48,49] and it is known that molecules deposited on Cu(111), Ag(111), and Au(111) can form complexes incorporating surface adatoms.[45,48−52] Wang et al.[49] demonstrated that an Ullmann-type coupling reaction performed on the Cu(111) surface resulted in the formation of a stable organometallic intermediate, with 4,4′-dibromo-*p*-terphenyl reacting to form a structure in which the *p*-terphenyl molecules are connected via a C−Cu−C bridge. In the system studied here, we propose that the steric repulsion between neighboring monomer units in the organometallic intermediate hinders the reductive elimination step of the Ullmann coupling reaction that results in the removal of the metallic atom and the covalent coupling of the adjacent carbon atoms.

The Au adatoms which form part of the organometallic complex are provided by the Au(111) surface. Au adatoms may potentially detach from the step edges, with the presence of iodine atoms on the Au(111) surface likely to enhance the mobility of the Au step-edge atoms,[47] leading to an increase in the number of mobile surface adatoms present at room temperature. Alternatively, the herringbone reconstruction of the Au(111) surface (where 23 surface atoms are compressed to fit the space of 22 bulk lattice sites[46]) has been shown to act as a source of Au adatoms, with the release of the metal atoms from the surface reconstruction facilitated by the adsorption of various chemical moieties,[53] including oxygen atoms,[54] NO_2,[55] Cl_2,[56] and thiols.[57] Adsorption of these molecules on the Au(111) surface gives rise, in all cases, to both a reordering of the herringbone reconstruction and the formation of adsorbate structures containing Au atoms. In the work performed by Maksymovych et al.,[57] alkane thiols were deposited on Au(111) and the removal of Au atoms from the surface combined with the localized lifting of the herringbone reconstruction was observed. The release of metal atoms from the surface reconstruction provided a reservoir of Au adatoms which were incorporated in the S−Au−S bonds observed within the organometallic structures formed on the surface.[57] Of particular interest to this work is the more general observation that the adsorption of electronegative elements, such as the halogen chlorine,[56] gives rise to the release of gold atoms from the herringbone reconstruction of the Au(111) surface, with the released atoms being incorporated into the adsorbate structure.[53] In our experimental data we observe a lifting of the herringbone reconstruction in the vicinity of the linear chains (shown in the STM image in Figure 2a; see also Supporting Information) which is likely to be due to release of Au atoms from the surface facilitated by the presence of the electronegative I atoms detached from the I_2TMTP molecules. We therefore infer that Au atoms released from the reconstruction via this mechanism are incorporated into the observed organometallic chains.

In our proposed structure for the linear chains, every I_2TMTP monomer unit is activated (i.e., the C−I bonds are dissociated) during annealing of the sample, resulting in activated 3,3″,5,5″-tetramethyl-1,1′:4′,1″-terphenyl (TMTP) species that allow each monomer to form two C−Au bonds to gold adatoms. Because of the steric interaction between the methyl groups of neighboring monomers within a chain, the terminal dimethyl-aryl rings of the TMTP monomers are forced to adopt either a *flat* or *tilted* adsorption geometry (indicated in Figure 2e). The flat ring geometry allows both of the methyl groups on the ring to be in contact with the Au(111) surface, whereas in the tilted orientation one methyl group is in contact with the surface while the other is lifted off the surface plane (colored red in Figure 2e). The calculations (Figure 2f) show that in STM images the tilted aryl rings should give rise to bright features within the molecular chain, while the flat rings should be imaged as darker features. This variation in molecular contrast is in excellent agreement with the structures observed in the STM experiments, an example of which is given in Figure 2g. In addition to the very good qualitative agreement between the images, the dimensions of the MM-calculated structure also agree well with the measured STM dimensions (compare experimental, L_0^{Exp}, L_1^{Exp}, L_2^{Exp}, and L_3^{Exp}, to calculated, L_0^{Calc}, L_1^{Calc}, L_2^{Calc}, and L_3^{Calc}, values in Figure 2d,e). Of particular note is the distance between two neighboring tilted rings (L_1^{Exp} = 6.1 ± 0.2 Å, L_1^{Calc} = 6.4 Å), which is in agreement with metal−organic bonds but at variance with the calculated value of 4.6 Å for the covalently linked model. The calculated MM structure for 2-unit chains (see Figure S7 of the Supporting Information) shows that the linking Au adatom is positioned 2.43 Å above the (111) surface plane, similar to the distance between two gold (111) planes in the bulk (2.46 Å), and in the approximate position expected for a Au adatom adsorbed at a 3-fold hollow site. For the 7-unit chain shown in Figure 2e, the registry with the surface is such that not all of the linking Au atoms are able to occupy 3-fold hollow sites on the surface; hence, some atoms are forced to adopt other positions. The average C−Au−C angle is found to be ∼165°, and the C−Au bond length is found to be 2.14 Å. The central aryl rings of each monomer lie 2.8 Å from the surface. The structure is stable in this intermediate state because of the substantial barrier for obtaining the covalently coupled reaction product, which is attributed to the steric repulsion between dimethyl-aryl rings.

The occurrence of such a complex yet periodic structure is not a priori obvious. One might expect a structure with "all flat" or "all tilted" rings to be energetically favored or that the energy

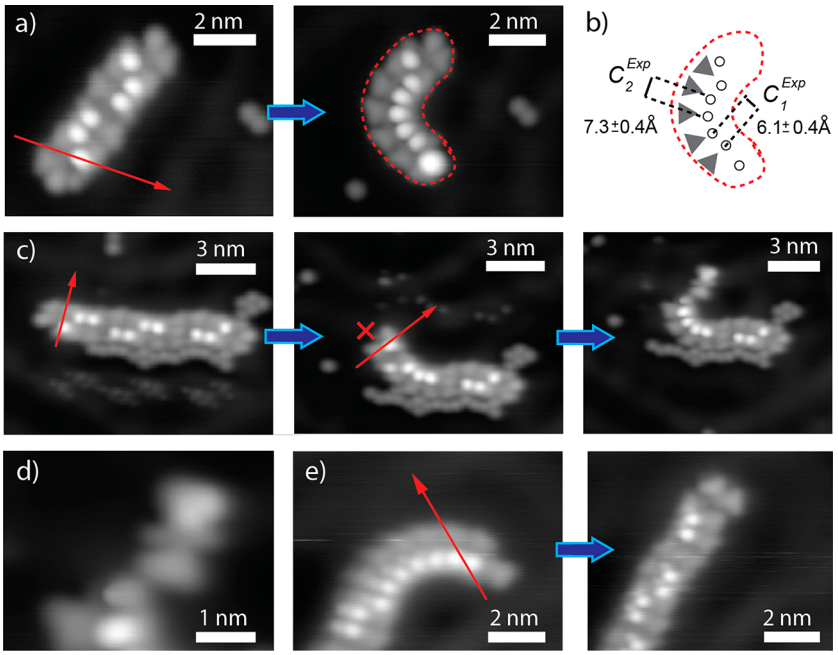

Figure 3. (a) STM images before and after the constant height lateral manipulation of a TMTP chain. Transition from a linear to a curved geometry is observed: the red arrow shows the path of the tip during the lateral manipulation. Imaging conditions: $V_{tip\text{-}bias}$ = −100 mV, I_{tunnel} = 100 pA. Manipulation conditions: $V_{tip\text{-}bias}$ = −100 mV, $I_{set\text{-}point}$ = 80 nA. (b) Schematic of the structure of a curved TMTP chain with the separation between the bright features (C_1^{Exp}) and the separation between monomer units (C_2^{Exp}) indicated. (c) A series of STM images taken during a constant-current manipulation experiment. The linear chain is laterally manipulated to produce a curved structure, with the red arrows showing the path of the tip during the manipulation. The red cross indicates the position from which two monomers have been detached. Imaging conditions: $V_{tip\text{-}bias}$= +500 mV, I_{tunnel} = 300 pA. Manipulation conditions: first manipulation step (red arrow in left STM image) $V_{tip\text{-}bias}$ = +10 mV, $I_{set\text{-}point}$= 8 nA; second manipulation step (red arrow in central STM image) $V_{tip\text{-}bias}$ = +10 mV, $I_{set\text{-}point}$ = 14 nA. (d) STM image showing a close-up of a monomer unit detached during the lateral manipulation shown in (c). Imaging conditions: $V_{tip\text{-}bias}$ = +50 mV, I_{tunnel} = 300 pA. (e) STM images taken before and after a constant current lateral manipulation. The red arrow shows the path of the tip during the lateral manipulation. Imaging conditions: $V_{tip\text{-}bias}$ = +100 mV, I_{tunnel} = 200 pA. Manipulation conditions: $V_{tip\text{-}bias}$ = +10 mV, $I_{set\text{-}point}$ = 14 nA.

landscape for the structure possesses a variety of minima that result in nonperiodic structures (i.e., random mixtures of flat and tilted adsorption geometries) along the chain. The MM calculations show that "all flat" or "all tilted" structures are not energetically favorable because of steric repulsion between neighboring rings in the case of "all flat" structures and the energy cost of lifting aryl rings away from the surface in the case of "all tilted" structures (see Supporting Information). The structure obtained by modeling a molecular chain of seven monomer units (Figure 2e,f) is potentially one of many energetically quasi-degenerate structures, and as such it is not possible to definitively identify it as the ground-state geometry (see Supporting Information for full discussion). However, the experimental finding that linear structures with the periodic arrangement of lobes along the chain are the dominant feature present on the surface suggests, together with the exceptional agreement between the ESQC-calculated STM image and the experimental data, that the calculated structure is the energetically most stable one.

It should be noted that the gold adatoms between two organic units are not visible in either the experimental or calculated STM images. As the distance between the monomer units is small, the STM signal of the metallic adatom is overshadowed by the signal of the rather large organic species. Such a finding has been previously observed for Ni adatoms incorporated within self-assembled PTCDI molecular structures on Au(111),[58] and Cu adatoms linking porphyrin compounds on Au(111).[45] It is however important to note (and in agreement with the explanation above) that gold atoms linked to isolated monomers, i.e., not within the organometallic linkage, can be identified (see below), similar to metallic adatoms at the termini of molecular chains.[58]

Via the combination of STM measurements, MM calculations, and ESQC-calculated images we are able to identify the adsorption geometry of individual monomers within the linear organometallic chains which give rise to the periodic arrangement of bright features along the polymers. We therefore observe three levels of ordering: (1) The adsorption geometry of the individual monomer units within the chain (being flat or tilted). (2) The conformational ordering of the chains (i.e., the periodic arrangement of monomer geometries). (3) The large-scale shape of the chain (straight and curved chains). In the following sections we shall discuss the interaction between the conformational ordering of the chains and their large-scale structure.

An interesting question is whether the shape of the polymer chains can be influenced by lateral manipulation with the STM tip. It has been shown in the last two decades by various groups that the lateral motion of the STM tip along a given pathway, either at constant tunneling current or at constant tip height,[2,3] can induce controlled changes to single molecules in terms of their adsorption site and geometry.[9−12] Figure 3a shows STM images acquired before and after the lateral manipulation of a short chain. It can clearly be seen that the shape of the chain is modified by the STM tip. The shape of the manipulated chain has changed from a straight to a curved geometry, which is similar to other cases.[16,50] Here, the conformational structure of the chain is also modified, which is evident from the change in

dx.doi.org/10.1021/jp409323g | J. Phys. Chem. C 2014, 118, 1719−1728

position of the bright features (tilted aryl rings) after bending. The majority of the bright features are now on the inside of the curved polymer, whereas before manipulation the bright features followed the periodic structure described above for the linear chain (out of 156 manipulation attempts 40 were successful, and all of these resulted in the bright features being arranged on the inside of the curved structure).

The apparent heights of the bright and dark features are 2.5 ± 0.2 and 1.5 ± 0.1 Å, respectively, which is in excellent agreement with the values for the linear chains. This finding indicates that the origin of the bright and dark features, i.e., tilted and flat dimethyl-aryl rings, is the same for both the linear and curved chains. The dimensions of the curved chain are shown in Figure 3b, with the distance between the tilted rings (C_1^{Exp}) found to be 6.1 ± 0.4 Å, in good agreement with the separation between neighboring bright features in the pairs of bright features observed within linear chains (L_1^{Exp}, 6.1 ± 0.2 Å). The separation between the centers of neighboring monomer units (C_2^{Exp}) is found to be 7.3 ± 0.4 Å.

Figure 3c shows a second example of the lateral manipulation of a linear chain, performed in two steps. The STM images show the structure of the chain before and after the lateral manipulation procedure. After the initial manipulation to produce a curved structure, one of the bright features has changed position from the bottom edge of the chain to the inside of the curve of the chain. It should also be noted that two monomer units have been detached (indicated by a red cross in Figure 3c) from the chain during manipulation, demonstrating the relatively fragile nature of the metal−organic bonding between the monomer units. The detachment of these monomer units gives further credence to the proposed model of the metal−organic linkages between the monomers,[50] as the manipulation of a covalently bonded chain via lateral manipulation would result in the displacement of the complete chain over the surface without any dissociation.[16] The flexibility and fragility of the chains is further demonstrated in the second step of the manipulation in Figure 3c where the chain is manipulated to induce a structure with an even smaller radius of curvature. In this case, a single monomer unit is detached from the chain during the manipulation and is visible in the final STM image (Figure 3c, close-up of detached monomer in Figure 3d). It is therefore difficult to repeatedly manipulate the chains without fragmentation because of the fragile nature of the metal−organic bonding. The detached monomer unit has a structure very similar to that observed for the intact molecules deposited onto a cold Au(111) surface (Figure 1). The length of the detached monomer (~18 Å) is in reasonable agreement with that for the intact monomers; the main difference is the absence of the bright protrusions corresponding to the iodine atoms, which are obviously not present in the case of the detached monomer. ESQC calculations show that the features on the sides of the detached monomer may be attributed to the Au adatoms that form part of the chain structure (see Supporting Information). The structure of the chain in Figure 3c, after the second lateral manipulation, is now highly curved at the left-hand side with four bright features (each corresponding to a tilted aryl ring) being on the inside curve of the chain. The overall structure is qualitatively similar to the curved structure seen in Figure 3a. Such manipulation events from linear to curved chain structures are highly reproducible. The change from a curved to a straight structure can also be studied; either starting with a "native" curved chain, i.e., not produced by manipulation (such as in Figure 3e), or with manipulated chains. Interestingly, it turns out that a characteristic periodic structure of bright features seen for the linear chain can be regained (Figure 3e; 6 out of 21 attempts were successful). The linear structure possesses a periodic arrangement of bright features similar to that observed for the native (nonmanipulated) linear chains, in agreement with our assignment that this is the energetically favored structure.

The structure of the curved chain (shown in Figure 4a) was modeled in the calculations at a temperature of 5 K, which is

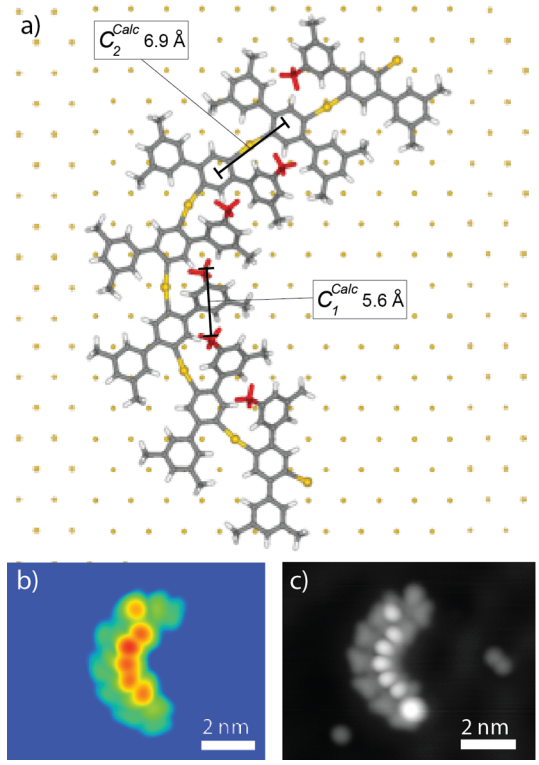

Figure 4. (a) Molecular-mechanics-calculated structure for the curved TMTP chain. (b) ESQC-calculated STM image showing a curved TMTP chain. (c) STM image of a curved TMTP chain produced via lateral manipulation ($V_{tip\text{-}bias}$ = −100 mV, I_{tunnel} = 100 pA).

similar to the temperatures during the STM experiments (around 6 K). In these "steered MD simulations", an additional force acting upon the central aryl ring of the monomer unit at one end of the chain, in a direction perpendicular to the backbone of the molecular chain (and parallel to the surface), is applied while the monomer at the other end of the oligomer is kept fixed. The applied force results in a bending of the molecular chain as the MD simulation evolves (see Supporting Information). The optimized structure for the curved chain (Figure 4a) clearly shows that on the outside of the chain all of the dimethyl-aryl rings are in the flat orientation.

On the inside, all dimethy-aryl rings are tilted by an angle (θ_{tilt}) of 40° relative to the surface plane to reduce the steric hindrance between the neighboring rings. In the calculated image (Figure 4b) the tilted rings are the brightest features, and the flat lying rings appear darker. The validity of the model is demonstrated by the striking agreement between the calculated STM image and the experimentally acquired data (in Figure 4b,c). The experimentally measured dimensions of the curved chain are also in reasonable agreement with the calculated dimensions (compare Figures 4a and 3b). Therefore, in both

dx.doi.org/10.1021/jp409323g | J. Phys. Chem. C 2014, 118, 1719−1728

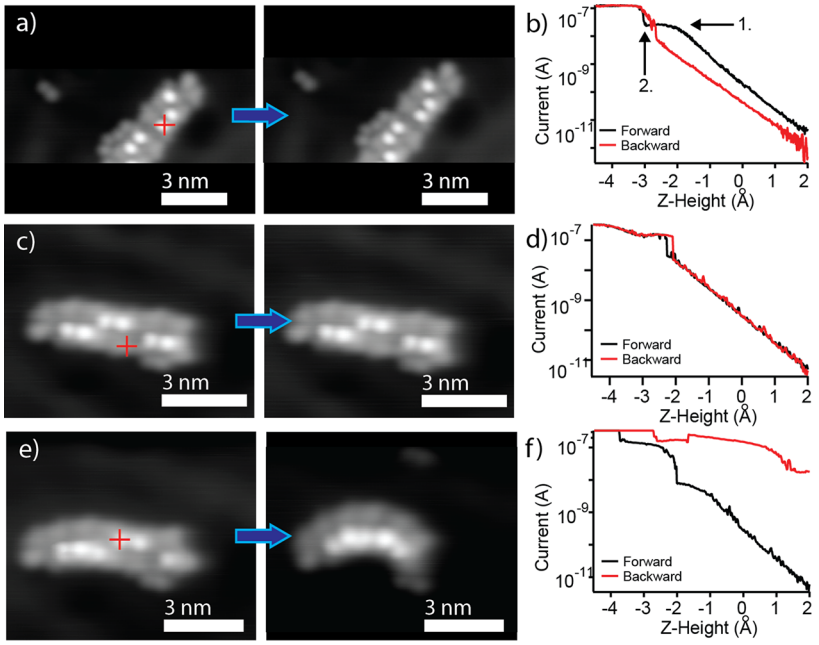

Figure 5. (a,c,e) STM images acquired before and after $I(z)$ spectroscopy. Imaging and spectroscopy conditions: $V_{tip\text{-}bias}$ = +50 mV, I_{tunnel} = 300 pA. The location of the tip-approach is indicated by a red cross. (b,d,f) Graphs showing the $I(z)$ data acquired from (a), (b), and (c) respectively.

cases (i.e., straight and curved chains) we may attribute the bright features to tilted dimethyl-aryl rings.

The MM calculations predict the curved structure (for a 7-unit oligomer) to be less stable (by 0.64 eV) than the linear structure, which is in agreement with the experimental observation that the majority (>90%) of the organometallic material assembled into chains on the surface is in a linear geometry. Constrained minimization and nudged elastic band calculations (for a 7-unit oligomer, see Supporting Information) were performed to obtain the energy barrier for transition between the linear and curved chains, with an activation barrier of 0.8 eV from linear to curved. This relatively large barrier for the transition accounts for the fact that no chains are observed to change from linear to curved structures during the STM measurements without undergoing lateral manipulation, due to the low thermal energy available at the low temperatures at which the experiments were conducted. Similarly, the low temperature of the molecule/substrate system stabilizes the energetically unfavorable curved chain structures produced by lateral manipulation.

The relationship between the large-scale shape of the chains (straight or curved) and the conformational structure of the chain (arrangement of bright features within the chain, which is related to the adsorption geometry of the monomers) can be understood in terms of a simple geometric model. For a self-assembled linear chain, a periodic arrangement for the adsorption geometries of the monomer units is adopted, with subsequent lateral manipulation of the chain giving rise to a curved shape (because of the flexibility of the molecular chain). The dimethyl-aryl rings on the outside of the curved structure are free to rotate and are able to lie flat on the metal surface (to maximize their interaction with the metal surface), giving rise to the dark features in the STM images. In contrast, the dimethyl-aryl rings on the inside of the curved chain are in close proximity to the neighboring rings and therefore interact strongly via steric repulsion. This interaction forces the rings on the inside of the chain to be tilted relative to the surface plane, resulting in the pattern of bright features observed in the STM images which is characteristic for the conformational structure of the curved chains.

In addition to lateral manipulation, it is also possible to interact with the polymer structures via vertical manipulation, i.e., approaching the tip perpendicular to the surface at a fixed lateral position.[11] The vertical manipulation of a bright feature within a linear TMTP chain is shown in Figure 5a,b. The STM images show a linear chain before and after vertical manipulation over a bright feature (the position of the tip approach over the chain is indicated by a red cross). The STM images before and after show no change to the overall structure of the chain or to the conformation of the monomer. However, it is possible to gain information about the process *during* the vertical manipulation by analyzing the measured current as a function of the STM tip position in real time ($I(z)$ trace in Figure 5b). The black line shows the measured current during the tip approach, with the initial slope of the curve revealing the expected exponential dependence of the tunneling current on the tip position. After the tip has approached about 2 Å toward the surface from the initial set-point, the gradient of the curve decreases, giving rise to a plateau region (arrow 1 in Figure 5b). Such a feature is indicative of a repulsive interaction between the tip and the underlying molecule where the molecule is pushed away from the tip, thus maintaining the same current.[11,12] In the present case, where the bright feature corresponds to a tilted dimethyl-aryl ring, we attribute this plateau in the $I(z)$ curve to the tilted aryl ring being pushed toward the surface, equivalent to previous work by Moresco et al.[12] Many such measurements (over 70) were performed for different bright features along the linear chains ($V_{tip\text{-}bias}$ = 50 mV, $I_{set\text{-}point}$ = 300pA), all exhibiting the same plateau at around −2 Å. In the final part of the $I(z)$ graph (at −3 Å, indicated by arrow 2) there is a sudden increase in the measured current (up to the point of saturating the preamplifier of the STM experiment) characteristic of the tip being in close contact with the molecule.

dx.doi.org/10.1021/jp409323g | J. Phys. Chem. C 2014, 118, 1719−1728

The $I(z)$ measurement for the subsequent tip retraction (red line in Figure 5b) shows a sudden change in the tunneling current at −2.5 Å with the slope showing the expected exponential dependence for tunneling through a vacuum. In various vertical manipulation experiments where the tip was approached between 2.5 and 3.8 Å toward the surface from the set-point, the approach and retract curves follow the same path. However, no change in the structure of the linear chain was observed in the subsequent image. This implies an important observation: although the position of the dimethyl-aryl ring was altered during the tip approach, the monomer unit returns to the same conformation during the tip retraction, demonstrating the stability of the periodic structure.

The same vertical manipulation procedure was performed over the dark features (flat aryl rings) along the length of the linear chains (shown in Figure 5c,d). The expected exponential increase in the through-vacuum tunneling was observed during the approach toward the molecule with a sudden increase in the measured current around −2 Å. The $I(z)$ traces show that both the approach and retraction curves have a sudden change in the measured current around −2 Å, similar to "jump to contact" features previously observed,[59] indicating that the tip interacts strongly with the molecule at distances less than −2 Å. The increase in current may be attributed to a change of molecular geometry within the tip−surface junction, with the "jump to contact" feature potentially being related to the flat aryl ring moving away from the surface (either by translation or rotation) to connect with the tip, providing an additional transport channel and giving rise to an increase in the measured current.[12] Upon retraction of the tip, through-vacuum tunneling is resumed with no change being observed in the structure of the chain in the subsequent STM image acquired after vertical manipulation.

In a minority of cases (about 10%) the vertical manipulation of a tilted dimethyl-aryl ring (bright feature) results in a more dramatic change of the structure of the linear chains. Examples where a linear chain is broken into two sections have been observed, and it is possible for the manipulation to induce a large-scale alteration of the molecular chain. One such interesting case is illustrated in Figure 5e,f where the vertical manipulation of one of the bright features within a linear chain results in the geometry of the chain switching from a linear to curved structure. The approach and retraction curves in Figure 5f show a form very different from that observed in Figure 5b, with the retraction curve in particular being substantially different from the approach curve. As is observed for all approaches above the bright features, the current trace exhibits a plateau around −2 Å, but in this case the curve is more complex and the retraction curve does not return to the original value of the current at the set-point (in agreement with the molecular changes). One possible explanation for this is that by changing the adsorption geometry of the dimethyl-aryl group beneath the tip from tilted to flat the internal energy of the structure has been increased because of the steric interactions between neighboring flat groups. To reduce the steric interactions, the shape of the chain may be forced to change from linear to curved, thus lowering the total energy of the structure. While the argument is consistent with our simple geometric model of the system, there is a second option which cannot be disregarded: the whole chain could be picked up by the tip during the manipulation and then dropped in a new curved structure. Because of the low number of occurrences of these rather large changes on an individual chain structure, a detailed analysis remains difficult.

The data obtained from the combination of STM imaging, vertical and lateral manipulation with the STM tip, and DFT, MM, and ESQC calculations discussed above demonstrate the link between the shape of the chain and its conformational structure. In summary: (1) More than 90% of the chain material observed on the surface after annealing is found to be in a linear geometry, all of which exhibits the periodic arrangement of bright features which is the signature of the conformational structure of the linear chains. (2) Of the 156 lateral manipulation attempts performed upon the linear chains, 40 were successful in producing curved structures (all of which exhibited the same regular arrangement of bright features on the inside curve of the chain, which is characteristic of the conformational structure for curved chains). (3) The lateral manipulation of a curved structure to a linear one results in the conformational structure returning to that which is characteristic for all linear chains. (4) The vertical manipulation of the adsorption geometry of a monomer unit within a linear chain (i.e., changing the conformational structure of the chain) is shown to result in a corresponding change in the shape of the chain from linear to curved.

CONCLUSIONS

We have demonstrated that it is possible to construct organometallic molecular chains via an on-surface synthesis process utilizing I_2TMTP molecules deposited on the Au(111) surface. The linear chains formed from a combination of TMTP monomers and gold adatoms have a highly periodic conformational structure over rather long distances, with pairs of bright features alternating along either side of the linear chain. A combination of STM experiments and calculations facilitates the identification of the bright and dark features within the chain as dimethyl-aryl rings of the monomer units either in tilted or flat adsorption geometries, respectively. The relationship between the adsorption geometries of the individual monomer units, the conformation of the chain, and the shape of the chains (linear or curved) is demonstrated by a series of lateral and vertical manipulation experiments. Changing the structure of a chain from linear to curved results in a corresponding transformation in the conformation of the chain, where the tilted dimethyl-aryl rings are all situated on the inside of the curved chain as opposed to the alternating structure observed for the linear chains. This finding demonstrates interdependence between the conformational structure and the large-scale geometry of the polymer. Vertical manipulation experiments reveal not only the intramolecular stability but also the energetic preference of the characteristic large-scale structure of the polymer chain.

ASSOCIATED CONTENT

Supporting Information

Details of the calculations, Extended discussion on the structure and manipulation of the linear and curved chains, Additional STM data on iodine characterization and disruption of the Au(111) herringbone reconstruction. This material is available free of charge via the Internet at http://pubs.acs.org.

AUTHOR INFORMATION

Corresponding Author

*E-mail: leonhard.grill@uni-graz.at. Phone: +43 316 3805412. Fax: +43 316 380 9850.

Author Contributions

A.S. performed the STM experiments. A.S. and L.G. analyzed the data. W.G. and X.B. carried out the theoretical calculations. G.F and A.G. carried out the molecular synthesis. L.G. and A.G. conceived the experiments. A.S. and L.G. wrote the manuscript. All authors discussed the results and commented on the manuscript.

Notes

The authors declare no competing financial interest.

■ ACKNOWLEDGMENTS

We are grateful for financial support from the European Project ARTIST. Part of this work was performed using High Performance Computing resources from the Calcul en Pyrénées (CALMIP) facilities (Grant 2011-[P0832]).

■ REFERENCES

(1) Eigler, D. M.; Schweizer, E. K. Positioning Single Atoms with a Scanning Tunnelling Microscope. *Nature* **1990**, *344*, 524−526.
(2) Stroscio, J. A.; Eigler, D. M. Atomic and Molecular Manipulation with the Scanning Tunneling Microscope. *Science* **1991**, *254*, 1319−1326.
(3) Bartels, L.; Meyer, G.; Rieder, K.-H. Basic Steps of Lateral Manipulation of Single Atoms and Diatomic Clusters with a Scanning Tunneling Microscope Tip. *Phys. Rev. Lett.* **1997**, *79*, 697−700.
(4) Bouju, X.; Joachim, C.; Girard, C. Single-Atom Motion During a Lateral STM Manipulation. *Phys. Rev. B: Condens. Matter Mater. Phys.* **1999**, *59*, R7845−R7848.
(5) Selvanathan, S.; Peters, M. V.; Schwarz, J.; Hecht, S.; Grill, L. Formation and Manipulation of Discrete Supramolecular Azobenzene Assemblies. *Appl. Phys.* **2008**, *93*, 247−252.
(6) Moresco, F. Manipulation of Large Molecules by Low-temperature STM: Model Systems for Molecular Electronics. *Phys. Rep.* **2004**, *399*, 175−225.
(7) Grill, L.; Moresco, F.; Jiang, P.; Joachim, C.; Gourdon, A.; Rieder, K. Controlled Manipulation of a Single Molecular Wire Along a Copper Atomic Nanostructure. *Phys. Rev. B: Condens. Matter Mater. Phys.* **2004**, *69*, 035416.
(8) Jung, T. A.; Schlittler, R. R.; Gimzewski, J. K.; Tang, H.; Joachim, C. Controlled Room-Temperature Positioning of Individual Molecules: Molecular Flexure and Motion. *Science* **1996**, *271*, 181−184.
(9) Beton, P. H.; Dunn, A. W.; Moriarty, P. Manipulation of C_{60} Molecules on a Si Surface. *Appl. Phys. Lett.* **1995**, *67*, 1075−1077.
(10) Grill, L.; Rieder, K.-H.; Moresco, F.; Rapenne, G.; Stojkovic, S.; Bouju, X.; Joachim, C. Rolling a Single Molecular Wheel at the Atomic Scale. *Nat. Nanotechnol.* **2007**, *2*, 95−98.
(11) Grill, L.; Rieder, K.-H.; Moresco, F.; Stojkovic, S.; Gourdon, A.; Joachim, C. Exploring the Interatomic Forces Between Tip and Single Molecules During STM Manipulation. *Nano Lett.* **2006**, *6*, 2685−2689.
(12) Moresco, F.; Meyer, G.; Rieder, K.-H.; Tang, H.; Gourdon, A.; Joachim, C. Conformational Changes of Single Molecules Induced by Scanning Tunneling Microscopy Manipulation: A Route to Molecular Switching. *Phys. Rev. Lett.* **2001**, *86*, 672−675.
(13) Alemani, M.; Gross, L.; Moresco, F.; Rieder, K.-H.; Wang, C.; Bouju, X.; Gourdon, A.; Joachim, C. Recording the Intramolecular Deformation of a 4-legs Molecule During Its STM Manipulation on a Cu(2 1 1) Surface. *Chem. Phys. Lett.* **2005**, *402*, 180−185.
(14) Matena, M.; Riehm, T.; Stöhr, M.; Jung, T. A.; Gade, L. H. Transforming Surface Coordination Polymers into Covalent Surface Polymers: Linked Polycondensed Aromatics through Oligomerization of N-Heterocyclic Carbene Intermediates. *Angew. Chem., Int. Ed.* **2008**, *47*, 2414−2417.
(15) Lafferentz, L.; Eberhardt, V.; Dri, C.; Africh, C.; Comelli, G.; Esch, F.; Hecht, S.; Grill, L. Controlling On-Surface Polymerization by Hierarchical and Substrate-Directed Growth. *Nat. Chem.* **2012**, *4*, 215−220.
(16) Lafferentz, L.; Ample, F.; Yu, H.; Hecht, S.; Joachim, C.; Grill, L. Conductance of a Single Conjugated Polymer as a Continuous Function of Its Length. *Science* **2009**, *323*, 1193−1197.
(17) McCarty, G. S.; Weiss, P. S. Formation and Manipulation of Protopolymer Chains. *J. Am. Chem. Soc.* **2004**, *126*, 16772−16776.
(18) Rauschenbach, S.; Vogelgesang, R.; Malinowski, N.; Gerlach, J. W.; Benyoucef, M.; Costantini, G.; Deng, Z.; Thontasen, N.; Kern, K. Electrospray Ion Beam Deposition: Soft-Landing and Fragmentation of Functional Molecules at Solid Surfaces. *ACS Nano* **2009**, *3*, 2901−2910.
(19) Dmitriev, A.; Spillmann, H.; Lin, N.; Barth, J. V.; Kern, K. Modular Assembly of Two-Dimensional Metal−Organic Coordination Networks at a Metal Surface. *Angew. Chem., Int. Ed.* **2003**, *42*, 2670−2673.
(20) Stepanow, S.; Lingenfelder, M.; Dmitriev, A.; Spillmann, H.; Delvigne, E.; Lin, N.; Deng, X.; Cai, C.; Barth, J. V.; Kern, K. Steering Molecular Organization and Host−Guest Interactions Using Two-Dimensional Nanoporous Coordination Systems. *Nat. Mater.* **2004**, *3*, 229−233.
(21) Classen, T.; Fratesi, G.; Costantini, G.; Fabris, S.; Stadler, F. L.; Kim, C.; de Gironcoli, S.; Baroni, S.; Kern, K. Templated Growth of Metal−Organic Coordination Chains at Surfaces. *Angew. Chem., Int. Ed.* **2005**, *44*, 6142−6145.
(22) Franc, G.; Gourdon, A. Covalent Networks through On-surface Chemistry in Ultra-High Vacuum: State-of-the-Art and Recent Developments. *Phys. Chem. Chem. Phys.* **2011**, *13*, 14283−14292.
(23) Heim, D.; Écija, D.; Seufert, K.; Auwärter, W.; Aurisicchio, C.; Fabbro, C.; Bonifazi, D.; Barth, J. V. Self-Assembly of Flexible One-Dimensional Coordination Polymers on Metal Surfaces. *J. Am. Chem. Soc.* **2010**, *132*, 6783−6790.
(24) Hart, H.; Harada, K.; Du, C. J. F. Synthetically Useful Aryl−Aryl Bond Formation via Grignard Generation and Trapping of Arynes. A One-Step Synthesis of *p*-Terphenyl and Unsymmetric Biaryls. *J. Org. Chem.* **1985**, *50*, 3104−3110.
(25) Smith, W.; Forester, T. R. DL_POLY_2.0: A General-Purpose Parallel Molecular Dynamics Simulation Package. *J. Mol. Graph.* **1996**, *14*, 136−141.
(26) Todorov, I. T.; Smith, W. DL_POLY_3: The CCP5 National UK Code for Molecular-Dynamics Simulations. *Philos. Trans. R. Soc., A* **2004**, *362*, 1835−1852.
(27) Mayo, S. L.; Olafson, B. D.; Goddard, W. A. DREIDING: A Generic Force Field for Molecular Simulations. *J. Phys. Chem.* **1990**, *94*, 8897−8909.
(28) Sutton, A. P.; Chen, J. Long-Range Finnis−Sinclair Potentials. *Philos. Mag. Lett.* **1990**, *61*, 139−146.
(29) Johnston, K.; Harmandaris, V. Properties of Benzene Confined Between Two Au(111) Surfaces Using a Combined Density Functional Theory and Classical Molecular Dynamics Approach. *J. Phys. Chem. C* **2011**, *115*, 14707−14717.
(30) Jónsson, H.; Mills, G.; Jacobsen, K. G. Nudged Elastic Band Method for Finding Minimum Energy Paths of Transitions. In *Classical and Quantum Dynamics in Condensed Phase Simulations*; Berne, B. J. et al. , Eds.; World Scientific: Singapore, 1998; p 388.
(31) Sautet, P.; Joachim, C. Calculation of the Benzene on Rhodium STM Images. *Chem. Phys. Lett.* **1991**, *185*, 23−30.
(32) Sautet, P.; Joachim, C. Electronic Transmission Coefficient for the Single-Impurity Problem in the Scattering-Matrix Approach. *Phys. Rev. B: Condens. Matter Mater. Phys.* **1988**, *38*, 12238−12247.
(33) Bouju, X.; Joachim, C.; Girard, C.; Tang, H. Mechanics of $(Xe)_N$ Atomic Chains Under STM Manipulation. *Phys. Rev. B: Condens. Matter Mater. Phys.* **2001**, *63*, 085415.
(34) Soe, W.-H.; Wong, H. S.; Manzano, C.; Grisolia, M.; Hliwa, M.; Feng, X.; Müllen, K.; Joachim, C. Mapping the Excited States of Single Hexa-peri-benzocoronene Oligomers. *ACS Nano* **2012**, *6*, 3230−3235.
(35) Landauer, R. Electrical Resistance of Disordered One-Dimensional Lattices. *Philos. Mag.* **1970**, *21*, 863−867.
(36) Bieri, M.; Nguyen, M.; Groning, O.; Cai, J.; Treier, M.; Ait-Mansour, K.; Ruffieux, P.; Pignedoli, C.; Passerone, D.; Kastler, M.; et al. Two-Dimensional Polymer Formation on Surfaces: Insight into

the Roles of Precursor Mobility and Reactivity. *J. Am. Chem. Soc.* **2010**, *132*, 16669−16676.
(37) Schlögl, S.; Heckl, W. M.; Lackinger, M. On-Surface Radical Addition of Triply Iodinated Monomers on Au(111)—The Influence of Monomer Size and Thermal Post-processing. *Surf. Sci.* **2012**, *606*, 999−1004.
(38) Eder, G.; Smith, E. F.; Cebula, I.; Heckl, W. M.; Beton, P. H.; Lackinger, M. Solution Preparation of Two-Dimensional Covalently Linked Networks by Polymerization of 1,3,5-Tri(4-iodophenyl)-benzene on Au(111). *ACS Nano* **2013**, *7*, 3014−3021.
(39) Blunt, M. O.; Russell, J. C.; Champness, N. R.; Beton, P. H. Templating Molecular Adsorption Using a Covalent Organic Framework. *Chem. Commun.* **2010**, *46*, 7157.
(40) Gutzler, R.; Walch, H.; Eder, G.; Kloft, S.; Heckl, W. M.; Lackinger, M. Surface Mediated Synthesis of 2D Covalent Organic Frameworks: 1,3,5-Tris(4-bromophenyl)benzene on Graphite(001), Cu(111), and Ag(110). *Chem. Commun.* **2009**, 4456.
(41) Lipton-Duffin, J. A.; Ivasenko, O.; Perepichka, D. F.; Rosei, F. Synthesis of Polyphenylene Molecular Wires by Surface-Confined Polymerization. *Small* **2009**, *5*, 592−597.
(42) Grill, L.; Dyer, M.; Lafferentz, L.; Persson, M.; Peters, M. V.; Hecht, S. Nano-Architectures by Covalent Assembly of Molecular Building Blocks. *Nat. Nanotechnol.* **2007**, *2*, 687−691.
(43) Koch, M.; Ample, F.; Joachim, C.; Grill, L. Voltage-Dependent Conductance of a Single Graphene Nanoribbon. *Nat. Nanotechnol.* **2012**, *7*, 713−717.
(44) Bieri, M.; Treier, M.; Cai, J.; Aït-Mansour, K.; Ruffieux, P.; Gröning, O.; Gröning, P.; Kastler, M.; Rieger, R.; Feng, X.; et al. Porous Graphenes: Two-Dimensional Polymer Synthesis with Atomic Precision. *Chem. Commun.* **2009**, 6919.
(45) Lin, T.; Shang, X. S.; Adisoejoso, J.; Liu, P. N.; Lin, N. Steering On-Surface Polymerization with Metal-Directed Template. *J. Am. Chem. Soc.* **2013**, *135*, 3576−3582.
(46) Barth, J. V.; Brune, H.; Ertl, G.; Behm, R. J. Scanning Tunneling Microscopy Observations on the Reconstructed Au(111) Surface: Atomic Structure, Long-Range Superstructure, Rotational Domains, and Surface Defects. *Phys. Rev. B: Condens. Matter Mater. Phys.* **1990**, *42*, 9307−9318.
(47) Huang, L.; Zeppenfeld, P.; Horch, S.; Comsa, G. Determination of Iodine Adlayer Structures on Au(111) by Scanning Tunneling Microscopy. *J. Chem. Phys.* **1997**, *107*, 585−591.
(48) Chung, K.-H.; Koo, B.-G.; Kim, H.; Yoon, J. K.; Kim, J.-H.; Kwon, Y.-K.; Kahng, S.-J. Electronic Structures of One-Dimensional Metal−Molecule Hybrid Chains Studied Using Scanning Tunneling Microscopy and Density Functional Theory. *Phys. Chem. Chem. Phys.* **2012**, *14*, 7304−7308.
(49) Wang, W.; Shi, X.; Wang, S.; Van Hove, M. A.; Lin, N. Single-Molecule Resolution of an Organometallic Intermediate in a Surface-Supported Ullmann Coupling Reaction. *J. Am. Chem. Soc.* **2011**, *133*, 13264−13267.
(50) Villagomez, C.; Sasaki, T.; Tour, J.; Grill, L. Bottom-up Assembly of Molecular Wagons on a Surface. *J. Am. Chem. Soc.* **2010**, *132*, 16848−16854.
(51) Björk, J.; Matena, M.; Dyer, M. S.; Enache, M.; Lobo-Checa, J.; Gade, L. H.; Jung, T. A.; Stöhr, M.; Persson, M. STM Fingerprint of Molecule−Adatom Interactions in a Self-Assembled Metal−Organic Surface Coordination Network on Cu(111). *Phys. Chem. Chem. Phys.* **2010**, *12*, 8815.
(52) Shi, Z.; Lin, N. Porphyrin-Based Two-Dimensional Coordination Kagome Lattice Self-Assembled on a Au(111) Surface. *J. Am. Chem. Soc.* **2009**, *131*, 5376−5377.
(53) Baker, T. A.; Kaxiras, E.; Friend, C. M. Insights from Theory on the Relationship between Surface Reactivity and Gold Atom Release. *Top. Catal.* **2010**, *53*, 365−377.
(54) Min, B. K.; Deng, X.; Pinnaduwage, D.; Schalek, R.; Friend, C. M. Oxygen-Induced Restructuring with Release of Gold Atoms from Au(111). *Phys. Rev. B: Condens. Matter Mater. Phys.* **2005**, *72*, 121410.
(55) Driver, S. M.; Zhang, T.; King, D. A. Massively Cooperative Adsorbate-Induced Surface Restructuring and Nanocluster Formation. *Angew. Chem., Int. Ed.* **2007**, *46*, 700−703.
(56) Gao, W.; Baker, T. A.; Zhou, L.; Pinnaduwage, D. S.; Kaxiras, E.; Friend, C. M. Chlorine Adsorption on Au(111): Chlorine Overlayer or Surface Chloride? *J. Am. Chem. Soc.* **2008**, *130*, 3560−3565.
(57) Maksymovych, P.; Sorescu, D. C.; Yates, J. T. Gold-Adatom-Mediated Bonding in Self-Assembled Short-Chain Alkanethiolate Species on the Au(111) Surface. *Phys. Rev. Lett.* **2006**, *97*, 146103.
(58) Yu, M.; Xu, W.; Kalashnyk, N.; Benjalal, Y.; Nagarajan, S.; Masini, F.; Lægsgaard, E.; Hliwa, M.; Bouju, X.; Gourdon, A.; et al. From Zero to Two Dimensions: Supramolecular Nanostructures Formed from Perylene-3,4,9,10-tetracarboxylic Diimide (PTCDI) and Ni on the Au(111) Surface through the Interplay Between Hydrogen-Bonding and Electrostatic Metal-Organic Interactions. *Nano Res.* **2012**, *5*, 903−916.
(59) Limot, L.; Kröger, J.; Berndt, R.; Garcia-Lekue, A.; Hofer, W. A. Atom Transfer and Single-Adatom Contacts. *Phys. Rev. Lett.* **2005**, *94*, 126102.